

ENDOGENOUS ELECTRIC FIELDS IN EMBRYOS DURING DEVELOPMENT, REGENERATION AND WOUND HEALING

R. Nuccitelli
RPN Research
144 Carroll St.
New Britain, CT 06053, USA

Abstract — All embryos that have been investigated drive ionic currents through themselves and these currents will generate internal electric fields. Here, those examples in which such fields have been measured directly are discussed. The first such measurements were made in chick embryos and about 20 mV mm^{-1} was measured near the posterior intestinal portal in 2–4-day-old embryos. This electric field is important for the development of tail structures because reducing its magnitude results in abnormal tail development. The second embryonic electric field measured directly was in the axolotl, where a rostral–caudal field of about the same magnitude was detected. Modification of this field during neurulation but not gastrulation caused developmental abnormalities. Most recently, the development of left–right asymmetry in frog and chick embryos was found to require a voltage difference between blastomeres at a very early developmental stage. This field was measured in the chick embryo to be $10\text{--}20 \text{ mV mm}^{-1}$ across the primitive streak. Mammalian skin wounds generate 150 mV mm^{-1} fields lateral to the wound and corneal epidermal wounds exhibit lateral fields of 40 mV mm^{-1} . The presence of these endogenous fields would suggest that exposures to external electric fields should be limited to magnitudes of less than 0.1 V m^{-1} .

INTRODUCTION

Essentially, every organ and cell in the human body uses electric voltage differences and ionic currents in the performance of critical daily functions. Every cell generates a voltage of roughly -70 mV across its outer membrane, which is used for a variety of signalling and transport functions. For example, retinal rod cells drive a relatively steady ‘dark current’ into the outer segment and out of the inner segment⁽¹⁾. This current is modulated as light is absorbed by rhodopsin in the outer segment to trigger a signal transduction cascade that reduces cGMP levels in the rod. Since the cGMP gates the Na^+ channels in the outer segment plasma membrane, this reduction in cGMP results in a reduction of the dark current and a consequent hyperpolarisation of the rod that influences vesicle secretion and signal transmission. Even cellular energy levels depend on voltage. All human cells make their universal energy currency, ATP, in large part by generating a 200 mV potential difference across the mitochondrial inner membrane. This theme continues in multicellular organs. Many organ functions are coordinated with electrical signals, such as the wave of depolarisation that sweeps over the heart to trigger a synchronous contraction to pump blood efficiently. Abnormalities in this electrical signal can lead to fibrillation and heart attacks. The voltages generated by the contracting heart are so large that they can be easily detected at the surface of the body and this signal, called the electrocardiogram or EKG, is routinely used to diagnose heart disease.

With this abundant use of electrical signals in cellular and organ function, it should not be a surprise that

endogenous electric fields are also important for normal development, regeneration and wound healing. This article outlines some of the more recent experimental findings in this area. Once the magnitude and time course of the natural, endogenous electric fields are known, a better informed judgment regarding the acceptable magnitude of external or environmental electric fields can be made.

ENDOGENOUS IONIC CURRENTS ARE PRESENT IN ALL CELLS AND TISSUES

The self-referencing probe has provided much information on the steady currents traversing cells and embryos

The author and Lionel Jaffe developed a technique for exploring transcellular ionic currents, called the vibrating or self-referencing probe⁽²⁾. This instrument vibrates a small platinum sphere between two points about $10 \mu\text{m}$ apart and measures the voltage between those points using signal averaging to improve the signal-to-noise ratio. In a conducting medium, where most cells find themselves, a voltage difference can only exist where there is a current flowing through the medium. Ionic currents entering or leaving cells can be readily detected by measuring the voltage that they generate as they flow through the extracellular medium and the past 30 years of research on more than 30 cell types has revealed that most cells have an asymmetrical distribution of ion channels that naturally leads to a transcellular current on the order of $1\text{--}10 \mu\text{A cm}^{-2(3,4)}$. The dark current in the retinal rod mentioned earlier results from the segregation of Na^+ channels to the outer segment and K^+ channels to the inner segment, combined with the high intracellular K^+ and low intracellular Na^+ produced by

the Na^+/K^+ -ATPase. This will result in an influx of Na^+ in the outer segment and efflux of K^+ from the inner segment, generating a transcellular 'dark' current. Rather than discuss all the cases of transcellular currents here, the reader is referring to previous reviews cited above. Here, on the electric field measurements made directly within developing embryos will be emphasised.

Both organs and embryos are surrounded by a monolayer of cells called an epithelium. Most epithelia exhibit a polarised distribution of ion channels that is similar to that found in the retinal rod and this leads to a similar transcellular current. However, this current cannot flow freely in the extracellular medium because these cells are attached to each other with both tight and adherens junctions. As the apical-basal transcellular current flows back extracellularly, it must follow a pathway between the cells, called a paracellular pathway (Figure 1). Current flow through this pathway encounters a high resistance region at the tight junctions near the apical end and the current flow through this resistance leads to a transepithelial potential that is positive on the basal side of the monolayer with respect to the apical side. The transepithelial potential (TEP) will be proportional to the resistance of this paracellular pathway and typical values for this TEP range from 15 to 60 mV, inside positive in human bodies. It is this TEP that is the driving force for most endogenous ionic currents in embryos and adults. This voltage across epithelia will drive current out of regions of low resistance, where there has been a break in the epithelium (wounds) or where tight junction resistance is low, such as along the primitive

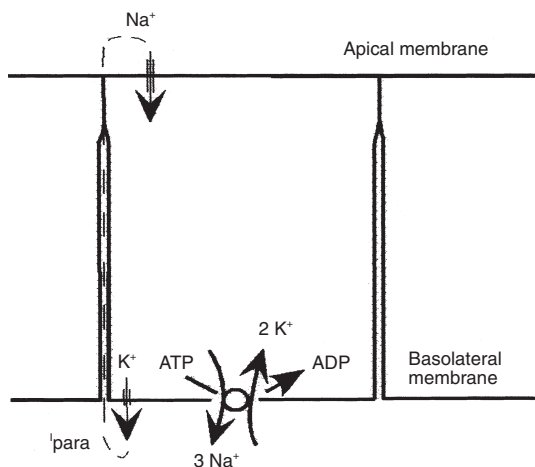


Figure 1. Diagram of a typical epithelial cell in a monolayer, with Na^+ channels localised on the apical plasma membrane and K^+ channels localised on the basolateral membranes, along with the Na^+/K^+ -ATPase. This asymmetric distribution of ion channels generates a transcellular flow of positive current that must flow back between the cells through the paracellular pathway (I_{para}). This current flow generates a transepithelial potential that is positive on the basolateral side of the monolayer.

streak^(5,6) or the posterior intestinal portal⁽⁷⁾ in chick or mouse embryos or at the forming limb bud in amphibian, chick and mouse embryos^(8–10). This 'leakage current' will, in turn, generate a lateral electric field along its path which will be proportional to the resistivity in that region. This electric field results from Ohm's law in a conductive medium, $E = J\rho$, where J is current density and ρ is the local resistivity. The earliest measurements of the leakage current associated with wounds were made more than a century ago. DuBois-Reymond⁽¹¹⁾ used a unique galvanometer that he built with more than 2 miles of wire and measured about 1 μA flowing out of a cut in one of his fingers. This was confirmed in 1849 and 1910 by other investigators and the history of these measurements is presented in a scholarly review by Venable⁽¹²⁾. More modern techniques have also been used to study this wound current. The 'leakage current' that is driven out of epithelia in low resistance regions has been measured using the vibrating probe technique⁽²⁾ in several systems. One of the earliest such measurements indicated a current as large as 100 $\mu\text{A cm}^{-2}$ leaving the stumps of regenerating new limbs⁽¹³⁾. Similar measurements have also been made on fingertip amputation currents in humans⁽¹⁴⁾ where up to 30 $\mu\text{A cm}^{-2}$ has been detected leaving the accidentally amputated stump for about 3 weeks. These currents will certainly generate electric fields just beneath the epidermis which will be proportional to the resistivity encountered in the tissue. The range of human tissue resistivity spans 200–1000 $\Omega \text{ cm}^{(15)}$, so these currents would be expected to generate an electric field within the tissue of about 10–100 mV mm^{-1} .

However, since this tissue resistivity can vary substantially as a function of cell density and tissue anatomy, it is always more reliable to measure these fields directly in the tissue rather than estimating them based on the transtissue current density. Such direct measurements of electric fields *in situ* have been made and these will be discussed next.

MEASUREMENTS OF ENDOGENOUS ELECTRIC FIELDS IN TISSUES AND EMBRYOS

The classic approach to these measurements is to use KCl filled glass microelectrodes to penetrate the outer epithelium and measure the voltage just beneath it in several positions. Another approach is to use voltage sensitive fluorescent dyes to report voltage differences associated with electric fields. Direct measurements of electric fields have been made in both avian and amphibian embryos during normal development. Hotary and Robinson⁽⁷⁾ used both the self referencing probe and microelectrodes to first detect the transembryonic current in the 2–4-day-old-chick embryo and then measure the electric field that the transembryonic current generates beneath the epidermis. They measured current entering much of the epidermis during stage 14 of development with the outward current focused mainly

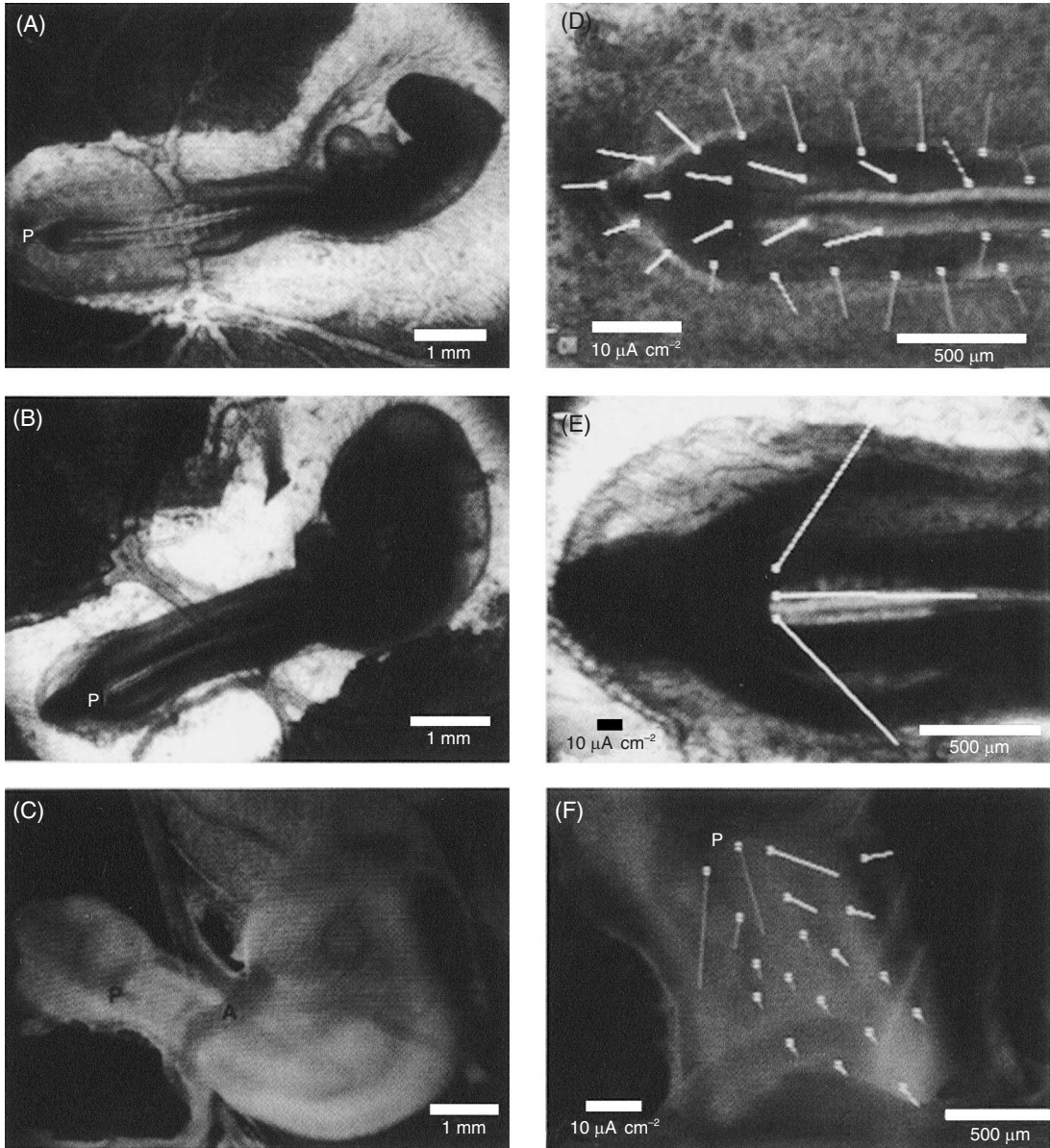


Figure 2. Ventral surface of three chick embryos at stage 14 (A and D), 17 (B and E) and 20 (C and F). Low magnification views of the whole embryo are shown in A–C while D–F show the current pattern around the posterior intestinal portals of the embryos. Current vectors are represented by lines originating at a dot that indicates the position of the self referencing probe when the measurement was made. The direction of the vector line away from the dot indicates the direction of current flow at that point and the length of the line is proportional to the current density. At stage 14 (D), all vectors point towards the posterior intestinal portal or the lateral walls of the midgut. The three vectors shown at stage 17 (E) indicate currents of about $100 \mu\text{A cm}^{-2}$ leaving the posterior intestinal portal. At stage 20 (F), outward currents were also found at the posterior intestinal portal. Current densities were much lower by this stage. Note the inward current at the anterior intestinal portal (A). (Reproduced from Reference 7, with permission from Elsevier.)

at the posterior intestinal portal, where up to $105 \mu\text{A cm}^{-2}$ was measured (Figure 2). One would expect that this large anterior–posterior current would generate an internal electric field so microelectrodes were then used to measure the TEP along this axis. Here, Hotary and Robinson measured electric fields of $5\text{--}20 \text{ mV mm}^{-1}$ and proceeded to test the hypothesis that these fields are important for normal development by perturbing them (Figure 3). They implanted a glass capillary that was filled with either conductive saline agar or non-conducting glass as a control through the ectoderm at the dorsal trunk of the embryo⁽¹⁶⁾. The conductive capillary allowed currents of about $5 \mu\text{A cm}^{-2}$ to leak out of the embryo. While the control embryos developed quite normally, most embryos with the implanted conducting capillary exhibited abnormalities in posterior structures where the endogenous electric field is normally the largest, but was reduced by the capillary shunt (Figure 4). Perturbing the normal voltage pattern within the embryo resulted in striking tail abnormalities and an investigation of a genetic mutant, *rumpleless*, which exhibits similar tail abnormalities led to a very interesting correlation. They found that most *rumpleless* mutants exhibited a much lower transembryonic current density and lower electric field within the embryo and those mutants that exhibited a normal electric field pattern also exhibited normal development. Therefore, they found a good correlation between the internal electric field and normal posterior development. These observations certainly support the hypothesis that the endogenous field is important for the development of posterior structures.

Similar work has been done on the stage 14–21 developing axolotl embryo⁽¹⁷⁾. Current is driven out of the lateral walls of the neural folds and the blastopore and enters most of the rest of the embryo's body surface (Figure 5). Measurements of the TEP indicate an internal, caudally negative electrical field beneath the neural plate ectoderm. The magnitude of the endogenous field is on the order of $10\text{--}20 \text{ mV mm}^{-1}$ (Figure 6). When these embryos were placed into an external electric field designed to modify the internal field, abnormalities were observed which depended on the developmental stage⁽¹⁸⁾. Gastrula stage embryos exhibited normal development after exogenous field exposure, indicating that the imposed field does not harm the embryo in some non-specific way. In contrast, neurula stage embryos exhibited developmental abnormalities when exposed to similar electric fields of $25\text{--}75 \text{ mV mm}^{-1}$. These data support the hypothesis that the natural electric field within the embryo influences normal morphogenesis.

The most recent study of the role of electric fields in development utilised both frog and chick embryos. The generation of left–right asymmetry in these systems was found to depend on both functioning gap junctions and a voltage difference between blastomeres in very early stages of development^(19–21). This work started with a pharmacological screen to identify drugs that interfered

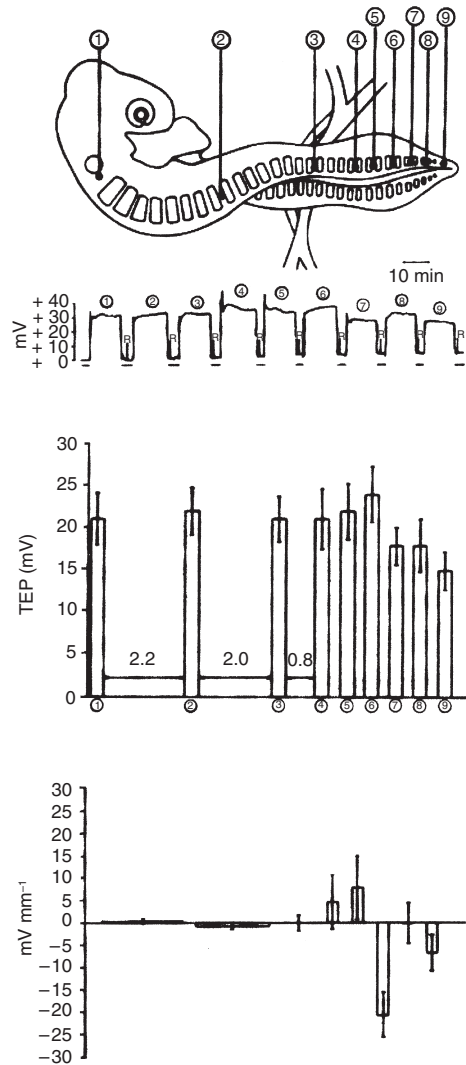


Figure 3. Stage 17 chick embryo TEP measured in nine rostral–caudal positions. Numbered measurement positions are shown in the drawing in the upper part of the figure. Below the drawing is a chart recording tracing, showing the TEP at the different measurement positions. At each numbered peak (corresponding to the positions shown in the drawing), the integument of the embryo was impaled and a stable positive potential was measured. Times at which the embryo was not impaled are indicated by a solid line below the recording. The upper bar chart shows the TEP at each position. The numbers below each bar correspond to the measurement positions indicated. The numbers between bars indicate the average distance (in mm) between each position. Where this is not indicated, the average distance is 0.3 mm. The lower chart shows the average voltage gradient between each consecutive position. Error bars indicate the SEM, $N = 6$. A steep voltage gradient was found between positions 6 and 7. (Reproduced from Reference 7 with permission from Elsevier.)

with the development of left–right patterning. The most effective drugs were ones that interfered with K^+ and H^+ ion fluxes. Lansoprazole and chromanol 293B were the most effective and block the H^+ pump and K^+ channel, respectively. The next most effective were SCH28080 and omeprazole, which block the H^+/K^+ -ATPase, followed by $BaCl_2$, which blocks K^+ channels. The hypothesis that these ion fluxes were important for left–right patterning was further tested by injecting mRNA for either the alpha or beta subunits of the H^+/K^+ -ATPase or the K^+ channel into the frog egg. It

was found that heterotaxia increased when either was injected but by far the largest increase (37%) occurred when all three mRNAs were injected. This suggests that overexpression of these molecules, which can influence or perturb ion concentration gradients of K^+ or H^+ , disrupted the normal left–right patterning of the embryo. In order to learn more about the mechanism through which H^+/K^+ -ATPase influenced patterning, *in situ* hybridisation was used to show an asymmetrical distribution of the K^+/H^+ -ATPase. It was concentrated in the right ventral blastomere of the 4 cell stage frog embryo.

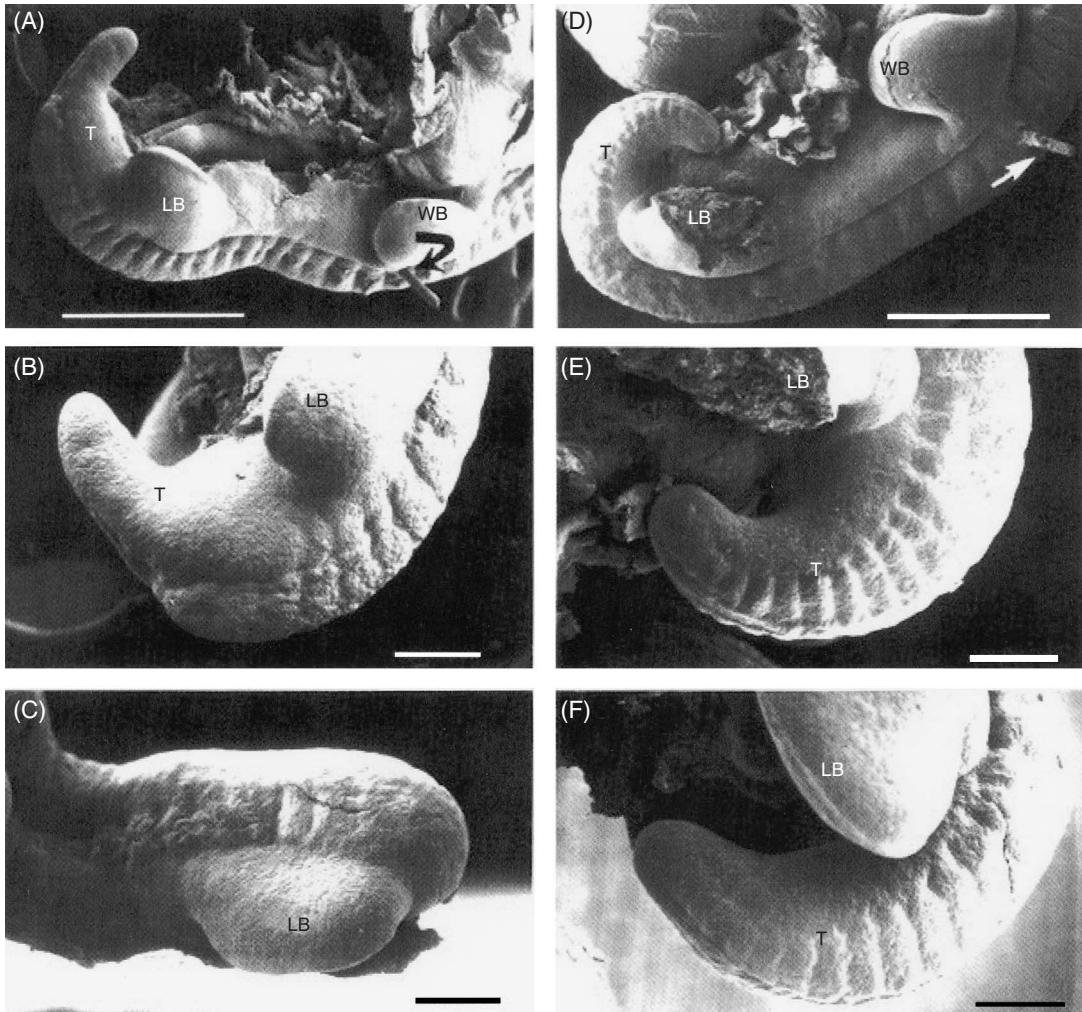


Figure 4. Scanning electron micrographs of experimental and control embryos. A and D show low magnification views of a current shunted (A) and a solid glass rod control (D) embryo. The arrows in each indicate the position of the implants near the level of the wing buds (WB). (B) Higher magnification of the tail region of the embryo shown in A. The tail (T) is nearly normal in length, but the distal half appears unstructured, lacking any somites or extension of the neural tube. (C) Experimental embryo that failed to develop a tail, terminating in a blunt stump just distal to the leg buds (LB). (E) Tail region of the solid rod control embryo shown in D. The leg bud has been partially removed in order to clearly visualise the normally formed tail. (F) Unoperated control embryo showing a normally formed tail. Scale bars: A, D = 1 mm; B, C, E and F = 250 μ m. (Reproduced from Reference 16, with permission from the Company of Biologists Ltd.)

Both additional K^+ channels and $H^+/K^+-ATPase$ will hyperpolarise cells, making them more negative than their neighbours. This voltage difference between the blastomeres of the 4 cell stage embryo could be used to segregate low molecular weight determinants through gap junctions to achieve asymmetric gene expression. This hypothesis was further tested by measuring the membrane potential of blastomeres during early chick development. An anionic fluorescent dye, DiBAC₄, was used whose distribution depended on membrane potential, to show that the early chick embryo exhibited a voltage gradient across the primitive streak. The left side of the primitive streak was 10–20 mV more positive than the right side and this difference was inhibited by the K^+ channel blocker, BaCl₂, and the $H^+/K^+-ATPase$ inhibitor, omeprazole (Figure 7). Since these drugs also partially inhibited the development of left–right patterning, the membrane potential difference appears to play a role in this aspect of development. This paper is the first to demonstrate a role for membrane potential differences between blastomeres in early vertebrate pattern formation. Another example of this occurs in early development of invertebrates, where a voltage across the cytoplasmic bridge is important for nurse cell–oocyte transport in the two moths, *Cecropia* and *Actius luna*^(22–24).

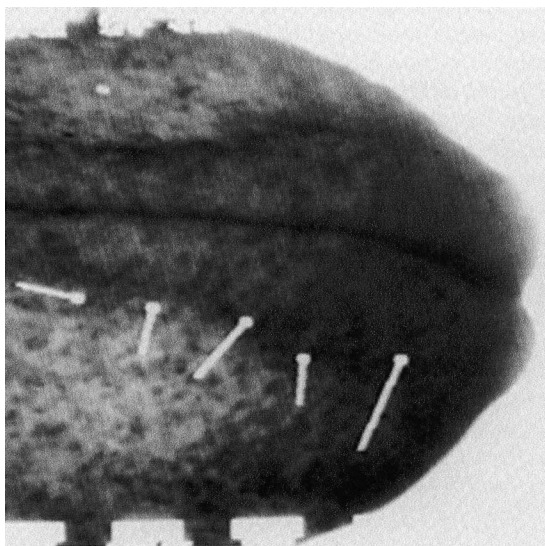


Figure 5. Neural fold currents in a stage 18 axolotl embryo measured with a 2-D self referencing probe. Current vectors are displayed as a line originating at a dot that marks the measurement position. The direction of current flow from the dot is denoted by the line direction and its length is proportional to the current density. Note the outwardly directed currents at the edge of the cranial neural folds. Reproduced from Reference 17, with permission from Wiley.

MEASUREMENTS OF ENDOGENOUS ELECTRIC FIELDS NEAR WOUNDS

Measurements of endogenous electric fields near epithelial wounds have been made in three different systems. The first was a skin wound in the guinea pig⁽²⁵⁾. The transepidermal potential was measured in several locations lateral to a skin wound. At the wound itself, there is no epidermis, so the transcutaneous potential is zero and, about 1 mm away, the transcutaneous potential exhibited the normal value of 50–70 mV. The steepest voltage gradient was found immediately adjacent to the wound edge, where values of about 150 mV mm⁻¹ were measured.

The second direct measurement of the electric field near a wound was made in two regions of the newt limb. The electric field adjacent to an amputated digit was measured with microelectrodes and found to be about 40 mV mm⁻¹^(26–28). This is very similar to the field near an amputated limb of the newt of 7–50 mV mm⁻¹⁽²⁸⁾.

The third direct measurement was made on the bovine cornea and the magnitude of the electric field there was 42 mV mm⁻¹^(29,30). The fields in the cornea and the newt digit have been found to play a role in wound healing. When the field strength is modified, the rate of wound healing changes. The newt's wound healing rate is optimised under normal conditions and cannot be speeded up, but removing the endogenous field does slow the rate of wound healing by about 25%. However, the rate of corneal wound healing can be enhanced by increasing the electric field strength. Epithelisation was

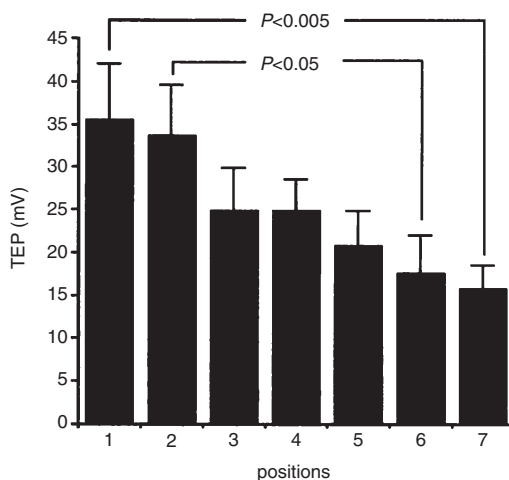


Figure 6. Rostral/caudal voltages beneath the neural plate in stage 16 axolotls. The magnitude of the neural plate TEP in eight embryos sampled at seven positions in the longitudinal axis is presented. Position 1 was the most rostral margin of the plate and fold, while position 7 was the most caudal, approximately 50 μ m from the blastopore. The statistical evaluation: Student's *t*, one tailed. Note the marked caudally negative slope in the electric potential. (Reproduced from Reference 17, with permission from Wiley.)

fastest in wounds with field strengths raised to -80 mV mm^{-1} , more than twice the normal field strength present in wounds maintained in Hanks' solution alone. Epithelialisation decreased, however, when the field strengths were increased to -120 mV mm^{-1} . A similar pattern was also observed when the field's polarity was reversed. Decreasing the field strength by submersion of the lesions or by treating the lesions with the Na^+ channel blocker, benzamil, significantly retarded healing. In addition, an increase in the field strength of lesions treated with Na^+ depleted Hanks' solution, by the

addition of direct current, increased the rate of epithelialisation. These observations suggest that the endogenous electric field is playing a role in the normal wound healing process.

ESTABLISHING GUIDELINES FOR EXOGENOUS ELECTRIC FIELD EXPOSURE

Based on these measurements of endogenous electric fields, it would be advisable to avoid exposures to external fields that might perturb the internal ones. The fields

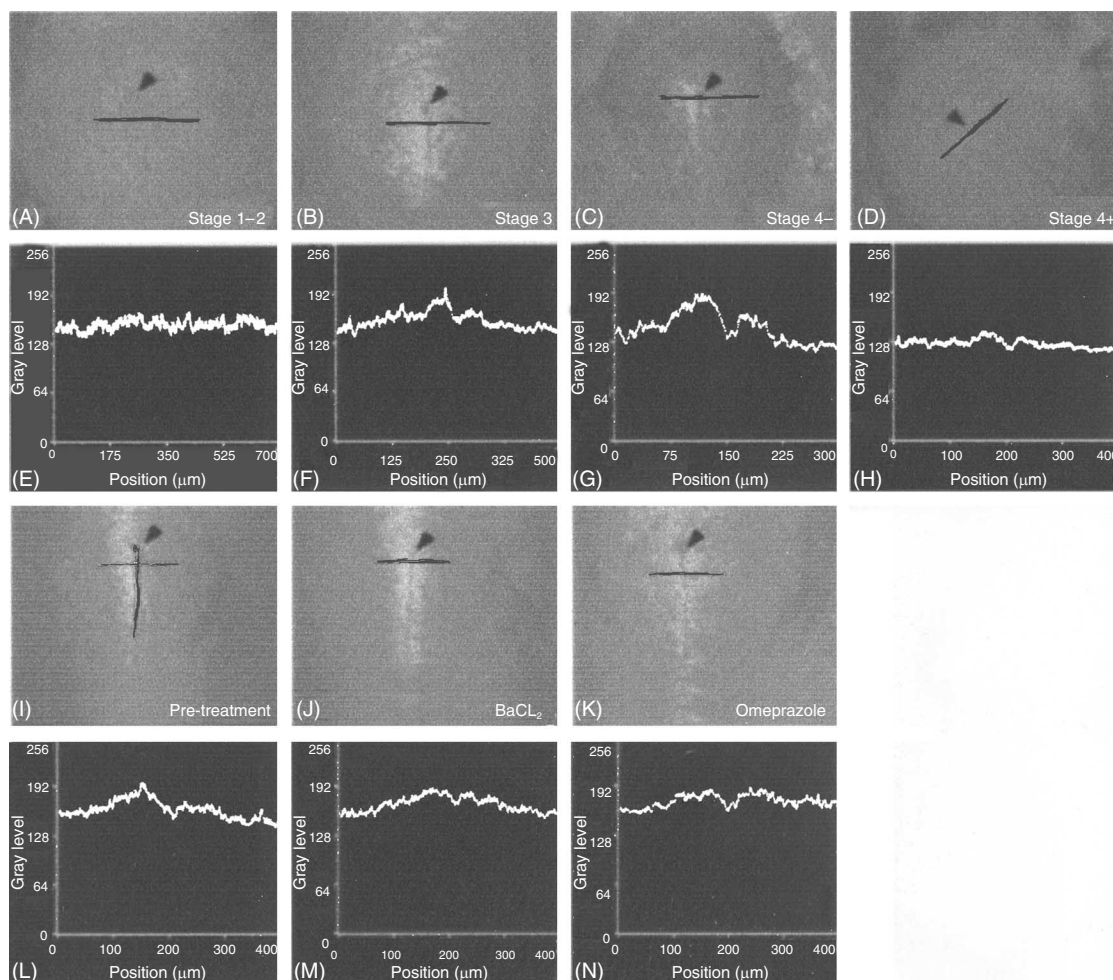


Figure 7. LR asymmetries of membrane potential patterns in the primitive streak area are modulated by BaCl_2 or omeprazole. (A–D) A transient domain of depolarisation to the left side of the primitive streak in chick embryos visualised with the potentiometric fluorescent probe, DiBAC₄. The blue to green to red pseudo-colour scale represents increasing fluorescence intensities, reflecting increased accumulation of the anionic dye in the intracellular membranes. Increased fluorescence corresponds to a less negative membrane potential. (E–H) Line scans of the embryos made perpendicular to the streak (red lines in A–D) show the increased left sided fluorescence. (I–K) Typical LR asymmetric pattern of depolarisation is seen prior to exposure (I). A relative increase in right sided fluorescence is seen in the same embryo as in 910 after exposure to BaCl_2 (J). Similar increase in right sided fluorescence after omeprazole exposure (K). Arrow heads indicated Hensen's node. (L–N) Line scans of the embryos (made along the red lines in I–K). (Reproduced from Reference 7, with permission from Elsevier.)

discussed here have all been steady, DC fields in the range of 10–150 mV mm⁻¹, and, because human bodies are conductors, external DC fields will not penetrate the body. However, higher frequency fields certainly can penetrate and a reasonable approach to take would be to limit exposure to fields so that the internal field generated would be less than 2 orders of magnitude lower than those normally present in our bodies. This would set the exposure limit to 0.1 V m⁻¹.

SUMMARY

All embryos that have been investigated drive ionic currents through themselves and these currents will generate internal electric fields as they traverse tissue. Cases in which such fields have been measured include:

1. the development of left–right asymmetry in frog and chick embryos utilises an electric field between blastomeres that is generated by an asymmetrical dis-

tribution of the K⁺/H⁺-ATPase among the blastomeres;

2. chick embryos, 2–4 days old, generate a 20 mV mm⁻¹ field near the posterior intestinal portal that is important for normal development of posterior structures;
3. stage 14–21 amphibian embryos generate similar internal electric fields and modifying these fields during neurulation but not gastrulation causes developmental abnormalities;
4. mammalian skin wounds generate 150 mV mm⁻¹ fields just below the stratum corneum and corneal epidermal wounds exhibit fields of 40 mV mm⁻¹ lateral to wounds.

Based on these measurements of internal endogenous electric fields, it would be prudent to avoid exposures to external fields that could significantly modify the natural ones. That would impose a limit of 0.1 V m⁻¹ induced inside the embryo from exposure to external fields.

REFERENCES

1. Hagins, W. A., Penn, R. D. and Yoshikami, S. *Dark currents and photocurrent in retinal rods*. Biophys. J. **10**, 380–412 (1970).
2. Jaffe, L. F. and Nuccitelli, R. *An ultrasensitive vibrating probe for measuring extracellular currents*. J. Cell Biol. **63**, 614–628 (1974).
3. Nuccitelli, R. *Ionic currents in morphogenesis*. Experientia **44**, 657–666 (1988).
4. Nuccitelli, R. The vibrating probe technique for studies of ion transport. In: *Noninvasive techniques in cell biology*. Eds J. K. Foskett and S. Grinstein (New York: Wiley-Liss) pp. 273–310 (1990).
5. Jaffe, L. F. and Stern, C. D. *Strong electrical currents leave the primitive streak of chick embryos*. Science. **206**, 569–571 (1979).
6. Winkel, G. K. and Nuccitelli, R. *Large ionic currents leave the primitive streak of the 7.5-day mouse embryo*. Biol. Bull. **176**, 110–117 (1989).
7. Hotary, K. B. and Robinson, K. R. *Endogenous electrical currents and the resultant voltage gradients in the chick embryo*. Dev. Biol. **140**, 149–160 (1990).
8. Robinson, K. R. *Endogenous electrical current leaves the limb and prelimb region of the Xenopus embryo*. Dev. Biol. **97**, 203–211 (1983).
9. Borgens, R. B., Rouleau, M. F. and DeLanney, L. E. *A steady efflux of ionic current predicts hind limb development*. J. Exp. Zool. **228**, 491–503 (1983).
10. Altizer, A. M., Moriarty, L. J., Bell, S. M., Schreiner, C. M., Scott, W. J. and Borgens, R. B. *Endogenous electric current is associated with normal development of the vertebrate limb*. Dev. Dyn. **221**(4), 391–401 (2001).
11. DuBois-Reymond, E. *Vorläufiger abriß einer untersuchung uber den sogenannten froschstrom und die electomotorischen fische*. Ann. Phys. U. Chem. **58**, 1 (1843).
12. Venable, J. W., Jr. *A history of bioelectricity in development and regeneration*. In: *A history of regeneration research*. Ed. C. E. Dinsmore (Cambridge: Cambridge University Press) pp. 151–177 (1991).
13. Borgens, R. B., Venable, J. W., Jr. and Jaffe, L. F. *Bioelectricity and regeneration: large currents leave the stumps of regenerating newt limbs*. Proc. Natl. Acad. Sci. USA **74**, 4528–4532 (1977).
14. Illingworth, C. M. and Barker, A. T. *Measurement of electrical currents emerging during the regeneration of amputated fingertips in children*. Clin. Phys. Physiol. Meas. **1**, 87–89 (1980).
15. Faes, T. J., van der Meij, H. A., de Munck, J. C. and Heethaar, R. M. *The electric resistivity of human tissues (100 Hz–10 MHz): a meta-analysis of review studies*. Physiol. Meas. **20**, R1–10 (1999).
16. Hotary, K. B. and Robinson, K. R. *Evidence of a role for endogenous electrical fields in chick embryo development*. Development **114**, 985–996 (1992).
17. Metcalf, M. E. M., Shi, R. Y. and Borgens, R. B. *Endogenous ionic currents and voltages in amphibian embryos*. J. Exp. Zool. **268**, 307–322 (1994).
18. Metcalf, M. E. M. and Borgens, R. B. *Weak applied voltages interfere with amphibian morphogenesis and pattern*. J. Exp. Zool. **268**, 323–338 (1994).

19. Levin, M. and Mercola, M. *Gap junctions are involved in the early generation of left–right asymmetry*. Dev. Biol. **203**, 90–105 (1998).
20. Levin, M. and Mercola, M. *Gap junction-mediated transfer of left-right patterning signals in the early chick blastoderm is upstream of Shh asymmetry in the node*. Development **126**, 4703–4714 (1999).
21. Levin, M., Thorlin, T., Robinson, K. R., Nogi, T. and Mercola, M. *Asymmetries in H⁺/K⁺-ATPase and cell membrane potentials comprise a very early step in left–right patterning*. Cell **111**, 77–89 (2002).
22. Jaffe, L. F. and Woodruff, R. I. *Large electrical currents traverse developing Cecropia follicles*. Proc. Natl. Acad. Sci. USA **76**, 1328–1332 (1979).
23. Woodruff, R. I. and Telfer, W. H. *Electrophoresis of proteins in intercellular bridges*. Nature **286**, 84–86 (1980).
24. Woodruff, R. I. and Cole, R. W. *Charge dependent distribution of endogenous proteins within vitellogenic ovarian follicles of Actias luna*. J. Insect Physiol. **43**, 275–287 (1997).
25. Barker, A. T., Jaffe, L. F. and Venable, J. W., Jr. *The glabrous epidermis of cavies contains a powerful battery*. Am. J. Physiol. **242**, R358–R366 (1982).
26. Chiang, M., Cragoe, E. J., Jr. and Venable, J. W., Jr. *Electrical fields in the vicinity of small wounds in Notophthalmus viridescens skin*. Biol. Bull. **176(S)**, 179–183 (1989).
27. Iglesia, D. D. S., Cragoe, E. J., Jr. and Venable, J. W., Jr. *Electric field strength and epithelization in the newt (Notophthalmus viridescens)*. J. Exp. Zool. **274**, 56–62 (1996).
28. McGinnis, M. E. and Venable, J. W., Jr. *Electrical fields in Notophthalmus viridescens limb stumps*. Dev. Biol. **116**, 184–193 (1986).
29. Chiang, M., Robinson, K. R. and Venable, J. W., Jr. *Electrical fields in the vicinity of epithelial wounds in the isolated bovine eye*. Exp. Eye Res. **54**, 999–1003 (1992).
30. Sta Iglesia, D. D. and Venable, J. W., Jr. *Endogenous lateral electric fields around bovine corneal lesions are necessary for and can enhance normal rates of wound healing*. Wound Repair Regen. **6(6)**, 531–542 (1998).

